Mathematical Modeling of Mitochondrial Adenine Nucleotide Translocase

Eugeniy Metelkin,* Igor Goryanin,† and Oleg Demin*
*A. N. Belozersky Institute of Physico-Chemical Biology, M. V. Lomonosov, Moscow State University, Moscow, Russia; and †University of Edinburgh, Appleton Tower, Edinburgh, United Kingdom

ABSTRACT We have developed a mathematical model of adenine nucleotide translocase (ANT) function on the basis of the structural and kinetic properties of the transporter. The model takes into account the effect of membrane potential, pH, and magnesium concentration on ATP and ADP exchange velocity. The parameters of the model have been estimated from experimental data. A satisfactory model should take into account the influence of the electric potential difference on both ternary complex formation and translocation processes. To describe the dependence of translocation constants on electric potential we have supposed that ANT molecules carry charged groups. These groups are shifted during the translocation. Using the model we have evaluated the translocator efficiency and predicted the behavior of ANT under physiological conditions.

INTRODUCTION

Adenine nucleotide translocase (ANT) catalyzes the electrogenic ATP and ADP exchange across the inner mitochondrial membrane. The transporter provides ATP efflux into the cytosol in exchange for ADP entering the matrix. It maintains a high concentration of ADP in mitochondria. It has been shown that ANT limits flux via oxidative phosphorylation under various conditions (1–4).

Despite the fact that ANT is one of the best-studied mitochondrial transport proteins (reviewed in 5–8), the kinetic mechanism and the composition of the functional unit are still under discussion. It is known that the antiporter operates in accordance with a 1:1 stoichiometry (9), carrying one ATP molecule for each ADP molecule, displaced in opposite directions. Two alternative schemes of the antiporter function have been proposed.

Klingenberg and co-authors (8,10) have proposed a one-site mechanism, where the ANT functional unit has one binding site facing either the matrix or the intramembrane space. It could be described by a ''ping-pong'' kinetic mechanism in accordance with Cleland's classification (11). However, studies of the dependence of the initial rate of ADP transfer on its concentration (12,13) have shown that the adenylate exchange mechanism is different from the ''ping-pong'' one. These facts led to the second hypothesis. In this scheme, the functional unit of the antiporter (6,7) contains two binding sites. This hypothesis has been confirmed by the fact that the functional unit of ANT is a homodimer (14). In this case, the two adenylate molecules bind to the ANT homodimer forming a ternary complex (two molecules of adenylate with the ANT homodimer), and then they are carried across the membrane in opposite directions. This conclusion is strongly consistent with recently performed x-ray structure analysis (15).

Using inhibition experiments, it has been shown that the binding sites of the ANT functional unit facing the internal and external sides of the membrane are different (14). Indeed, bongkrekic acid attacks the part of the protein facing the matrix, whereas atractiloside binds to the protein helices exposed to the intramembrane space. This demonstrates the anisotropy of the ANT functional unit with respect to the inner mitochondrial membrane.

Few mathematical models describing ANT kinetics have been published so far. The model of Kraemer and Klingenberg (10) was designed according to the one-site hypothesis of antiporter function. They determined other parameters of the rate equation using experimental values of the apparent K_m and V_{max} . In addition, they demonstrated that the rate constants of transmembrane transfer depend significantly on the membrane potential, whereas the association/dissociation constants remain the same under 0–180 mV variation of the potential. As we mentioned earlier, such models with one binding site per functional unit fit the kinetic experiments poorly and cannot explain data from Duyckaerts et al. (12) and Barbour and Chan (13).

A mathematic model based on a two-site functional mechanism has been built by Aliev and Saks (5). In the framework of their model, apparent parameters K_m and V_{max} have been expressed in terms of parameters of the two-site model. The authors estimated parameters of the model from apparent K_m and V_{max} values measured experimentally (10). Using the model, the authors (5) successfully described experimental data qualitatively (12,13). However, the proposed composition of the antiporter functional unit is inconsistent with the recent x-ray structure data (15). Moreover, the model did not take into consideration the anisotropy of the functional unit of the ANT and it did not match with the experimental data on specific inhibitor binding.

Although both models enabled the authors to estimate kinetic parameters corresponding to values of the transmembrane potential difference equal to 0 mV and 180 mV, none of them used the transmembrane potential explicitly in

Submitted February 26, 2005, and accepted for publication September 7, 2005.

Address reprint requests to Eugeniy A. Metelkin, Moscow State University, Leninskie Gory, Moscow, Russia 119992. Fax: 7-095-939-3181; E-mail: metelkin@insysbio.ru.

0006-3495/06/01/423/10 $2.00

doi: 10.1529/biophysj.105.061986

the rate equation. As a consequence, the carrier behavior under conditions other than the experimental ones has not been explained. This problem has been addressed in the model proposed by Kholodenko (4,16,17). The model suggested the existence of two binding sites for each transporter's functional unit. Electric potential influence on kinetic constants was taken into consideration, but the model was mostly empirical and the modeling results were not compared with any experimental data.

Our analysis revealed several drawbacks in the models described above:

1. Existing ANT models are not entirely based on known structural and functional information. For instance, the models published so far are not able to reproduce some of the experimental data even qualitatively.
2. Different types of experimental data have been explained by different ANT models. So, no unique set of parameters has been identified.
3. Parameters have been calculated on the basis of apparent, but not directly measured, experimental values of K_m and V_{max} . This could lead to the large errors in parameter estimations.
4. The influence of electric fields on ANT function either has not been taken into account or has been described empirically using the typical assumptions in most of the models published so far. The theoretical basis of empirical approaches has not been properly developed.
5. No model has explained the experimentally proven fact that ANT catalyzed exchange rate depends on pH (9).

In this study, we develop the ANT model and address the problems indicated above. The goal is to design a valid kinetic model of mitochondrial adenine nucleotide translocase on the basis of all currently available structural and functional information. We describe the dependence of the exchange rate on membrane potential using not empirical but physical considerations. The adenylate distributions on either side of the membrane have also been taken into account. The other purpose of our study is a methodological one. We propose a new approach to describing the dependence of reaction rates on membrane potential.

Using the model we have predicted how the rate of the ATP/ADP translocation depends on adenine nucleotide concentrations, pH, and electric potential difference under conditions close to the physiological. We have determined how the effectiveness of ANT operation is controlled by adenylate concentrations and potential.

MODEL DESIGN

Experimental data for model verification

To develop and verify the kinetic model of ANT we used experimental data from Kraemer and Klingenberg (10). To characterize exchange kinetics they used translocator reconstructed into liposomes. This experimental technique enabled them to avoid the influences of other intramitochondrial components and the inhibitory effects of bivalent cations. It allowed the authors to measure the dependence of the initial rates of labeled adenylate influx on their bulk phase concentration at different concentrations of internal adenylate, pH, and membrane potential. We have used the results of the original study to verify our model and estimate its parameters. It is worth mentioning that in all of the experiments, ATP and ADP concentrations inside liposomes were much higher than the dissociation constants of internal ANT binding sites. This allowed us to estimate only the ratio of dissociation constants for ATP and ADP, but not the values themselves.

Antiporter functional mechanism

Here, we assumed that the adenine nucleotide translocase functional unit is a dimer operating as two mutually concerted channels transporting two molecules of adenylates in opposite directions. As the subunit properties are anisotropic, i.e., there are different binding sites of the protein to associate with the adenylates, one facing the mitochondrial matrix and one the intramembrane space (15), two possible mechanisms could be proposed. Fig. 1 illustrates these possible arrangements of the subunits in the dimer. The *trans* scheme (Fig. 1 *A*) refers to the situation where adenylate binding sites for the monomers on each side of the membrane are the same in either state of the antiporter functional unit. If the *trans* scheme were realized, the transporter's dimer in any state would have the same properties on each side of the membrane, which would be inconsistent with the ANT anisotropy property (14). For this reason, the *cis* scheme of the location (Fig. 1 *B*) is more likely, because in any state the transporter has only one type of binding site on each side of the membrane.

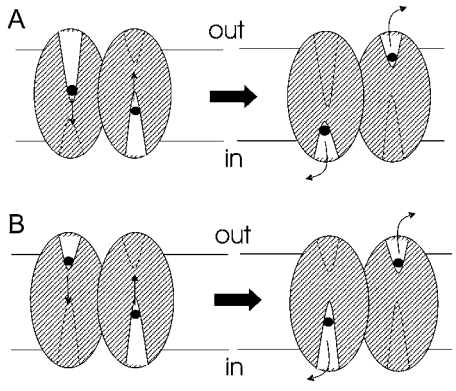

FIGURE 1 Possible position of the subunits in the functional unit of ANT. (*A*) Isotropic position of the *trans* type: both sides of the membrane are identical for binding and transfer. (*B*) Anisotropic position of the *cis* type: there is only one type of site on each side of the membrane.

Kinetic scheme

In accordance with the functional mechanism (*cis* scheme, Fig. 1 *B*) of ANT chosen in previous section we propose an appropriate kinetic scheme (depicted in Fig. 2) as the most probable one. This scheme corresponds directly to the ''Bi-Bi Random'' mechanism in Cleland's classification (11). Two stages are involved in the formation of the ternary complexes between the antiporter and adenylates (*TET*, *TED*, *DET*, and *DED*). As shown in Fig. 2, ATP or ADP binds to sites of ANT facing either side of the membrane (dissociation constants are indicated by the corresponding reactions). Formation of the complexes induces the transfer of adenylates in opposite directions and dissociation afterward to leave binding sites available for the next cycle. Rate constants of each elementary transfer stage are shown in the scheme. Rate constants k_2 and k_3 describe rates of direct and indirect exchange of ATP for ADP. Rate constants k_1 and k_4 correspond to exchange of identical adenylates (ATP for ATP or ADP for ADP) described in the work of Kraemer and Klingenberg (10).

Derivation of the rate equation

To simplify the process of model construction and analysis we assumed that

1. The association/dissociation stages of the ANT catalytic cycle (Fig. 2, *lines*) are in a quasiequilibrium state. This directly corresponds to the approximation suggested by Kraemer and Klingenberg (10) that transmembrane adenylate transfer (Fig. 2, *arrows*) limits ANT function.
2. ANT is able to carry only deprotonated and magnesium-free forms of adenylates. Indeed, there are few forms of adenylates found in vivo, because ATP and ADP can be protonated and bound with bivalent cations (mainly with magnesium). However, it was previously shown that the magnesium forms are not involved in exchange catalyzed by ANT (8,18). This conclusion is consistent with the well known inhibitory role of magnesium cations for the antiporter. Furthermore, it has been demonstrated that only ADP and ATP molecules carrying the charges 3− and 4−, respectively, were able to be transferred across the membrane (7,9).
3. The electrostatic field of the charged membrane influences both the stage of transfer and the stage of ternary complex formation. We accommodate the most general case of interactions between the electric field of membrane and molecules taking part in translocation. Such interactions will be described via dependencies of kinetic parameters on the potential difference of the membrane.

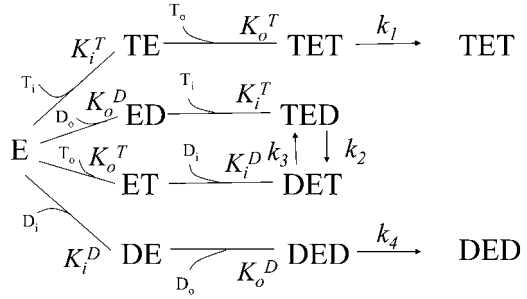

FIGURE 2 Kinetic scheme of the catalytic cycle of the mitochondrial ANT. *T* and *D* are understood as ATP and ADP, respectively, the subscripted index indicating the location: *i*, inside the matrix; and *o*, within the intramembrane space. *E* is the free form of the enzyme. *XEY* is a ternary complex of an ANT dimer with molecules *X* from the matrix and *Y* from the intramembrane space. Lines show processes of complex formation. Arrows show transfer processes. The scheme shows the constants of the transfer rates and dissociation constants for the corresponding stages.

According to the scheme of the catalytic cycle, the full turnover number per unit of time may be expressed as follows:

$$v = k_1\,TET + k_2\,TED + k_3\,DET + k_4\,DED, \tag{1}$$

where *TET*, *TED*, *DET*, and *DED* are concentrations of the corresponding antiporter states with respect to the internal volume of liposomes, i.e. the ratio of the number of molecules in each state to the volume of liposomes. The concentrations in different states may be expressed in terms of adenylate concentrations using equilibrium relationships corresponding to association/dissociation stages:

$$\begin{aligned} &TE = E\frac{T_\mathrm{i}}{K_\mathrm{i}^\mathrm{T}}, \quad ED = E\frac{D_\mathrm{o}}{K_\mathrm{o}^\mathrm{D}}, \quad ET = E\frac{T_\mathrm{o}}{K_\mathrm{o}^\mathrm{T}}, \quad DE = E\frac{D_\mathrm{i}}{K_\mathrm{i}^\mathrm{D}},\\ &TET = E\frac{T_\mathrm{i}T_\mathrm{o}}{K_\mathrm{i}^\mathrm{T}K_\mathrm{o}^\mathrm{T}}, \quad DET = E\frac{D_\mathrm{i}T_\mathrm{o}}{K_\mathrm{i}^\mathrm{D}K_\mathrm{o}^\mathrm{T}}, \quad TED = E\frac{T_\mathrm{i}D_\mathrm{o}}{K_\mathrm{i}^\mathrm{T}K_\mathrm{o}^\mathrm{D}},\\ &DED = E\frac{D_\mathrm{i}D_\mathrm{o}}{K_\mathrm{i}^\mathrm{D}K_\mathrm{o}^\mathrm{D}}, \end{aligned} \tag{2}$$

where *T* and *D* refer to concentrations of deprotonated adenylates (ATP and ADP, respectively). The subscripted indices *o* and *i* imply their location—*o* outside the liposome and *i* inside the liposome. The concentration of the free form of transporter *E* may be derived from the equation expressing the total ANT concentration as the sum of concentrations of its different states:

$$E + TE + ET + DE + TET + DET + TED + DED = E_0. \tag{3}$$

By rearranging Eqs. 1–3, we obtain

$$E = E_0/\Delta,$$

where

$$\begin{aligned} \Delta &= 1 + \frac{T_\mathrm{i}}{K_\mathrm{i}^\mathrm{T}} + \frac{T_\mathrm{o}}{K_\mathrm{o}^\mathrm{T}} + \frac{D_\mathrm{i}}{K_\mathrm{i}^\mathrm{D}} + \frac{D_\mathrm{o}}{K_\mathrm{o}^\mathrm{D}} + \frac{T_\mathrm{i}T_\mathrm{o}}{K_\mathrm{i}^\mathrm{T}K_\mathrm{o}^\mathrm{T}} + \frac{D_\mathrm{i}T_\mathrm{o}}{K_\mathrm{i}^\mathrm{D}K_\mathrm{o}^\mathrm{T}}\\ &\quad + \frac{T_\mathrm{i}D_\mathrm{o}}{K_\mathrm{i}^\mathrm{T}K_\mathrm{o}^\mathrm{D}} + \frac{D_\mathrm{i}D_\mathrm{o}}{K_\mathrm{i}^\mathrm{D}K_\mathrm{o}^\mathrm{D}} = \left(1 + \frac{T_\mathrm{o}}{K_\mathrm{o}^\mathrm{T}} + \frac{D_\mathrm{o}}{K_\mathrm{o}^\mathrm{D}}\right)\left(1 + \frac{T_\mathrm{i}}{K_\mathrm{i}^\mathrm{T}} + \frac{D_\mathrm{i}}{K_\mathrm{i}^\mathrm{D}}\right),\\ v' &= \frac{v}{E_0} = \frac{1}{\Delta}\left(k_1\frac{T_\mathrm{i}T_\mathrm{o}}{K_\mathrm{i}^\mathrm{T}K_\mathrm{o}^\mathrm{T}} + k_2\frac{T_\mathrm{i}D_\mathrm{o}}{K_\mathrm{i}^\mathrm{T}K_\mathrm{o}^\mathrm{D}} + k_3\frac{D_\mathrm{i}T_\mathrm{o}}{K_\mathrm{i}^\mathrm{D}K_\mathrm{o}^\mathrm{T}} + k_4\frac{D_\mathrm{i}D_\mathrm{o}}{K_\mathrm{i}^\mathrm{D}K_\mathrm{o}^\mathrm{D}}\right), \end{aligned} \tag{4}$$

where ν' is the full turnover number for a single functional unit of ANT per unit of time. To estimate parameters of the equation we fitted it against experimentally measured dependencies of initial exchange rate on concentration of external adenylates (10). Since these dependencies have been measured in conditions where the concentration of inner adenylates is much higher than the dissociation constants of the binding site facing the internal space of the liposome, the following inequality is true:

$$T_i/K_i^T + D_i/K_i^D \gg 1.$$

By using the inequality, we can simplify the denominator Δ of Eq. 4:

$$\Delta \cong \left(1 + \frac{T_o}{K_o^T} + \frac{D_o}{K_o^D}\right)\left(\frac{T_i}{K_i^T} + \frac{D_i}{K_i^D}\right).$$

Multiplying numerator and denominator of Eq. 4 by K_i^D we can reduce the number of parameters by one:

$$v' = \frac{1}{\Delta'}\left(k_1 q\frac{T_i T_o}{K_o^T} + k_2 q\frac{T_i D_o}{K_o^D} + k_3\frac{D_i T_o}{K_o^T} + k_4\frac{D_i D_o}{K_o^D}\right),$$
$$\Delta' = \Delta \times K_i^D = \left(1 + \frac{T_o}{K_o^T} + \frac{D_o}{K_o^D}\right)(D_i + qT_i), \qquad (5)$$

where $q = K_i^D/K_i^T$ is the affinity ratio of the internal ANT binding site for ATP and ADP.

Equation 5 represents the turnover rate of the antiporter. It describes both the ''productive cycles'' (exchange of ATP for ADP) and ''futile cycles'' (exchange of ATP for ATP or ADP for ADP). Since each turnover results in an adenylate molecule being carried across the membrane, Eq. 5 describes the dependence of the influx rate of the labeled adenylates on their external and internal concentrations. These dependencies have been measured by Kraemer and Klingenberg (10) and we use them to identify the unknown parameters of the model.

To describe ANT function in mitochondria we derive an equation for the rates of change in adenylate concentrations (not turnover rate!) as a function of their matrix and intermembrane space concentrations. This means that only ''productive cycles'' of ANT should be taken into account. Since the stoichiometry of ANT is 1:1, the ADP concentration change is equal to that of ATP but with the opposite sign.

$$\frac{dD_i}{dt} = -\frac{dT_i}{dt} = v_{exchange},$$

where $v_{exchange}$ stands for the exchange rate, i.e., the rate of the changes in adenylate concentrations.

According to the scheme of the ANT catalytic cycle (Fig. 2), the exchange rate can be expressed as follows:

$$v_{exchange} = k_2\, TED - k_3\, DET.$$

This equation takes into account only ''productive cycles'', i.e., those resulting in exchange of ATP for ADP but not ATP for ATP or ADP for ADP. Similarly to Eqs. 1–5, we can derive the exchange rate per dimer of ANT as a function of concentrations of adenylates and the kinetic parameters.

$$v'_{exchange} = \frac{1}{\Delta'}\left(k_2 q\frac{T_i D_o}{K_o^D} - k_3\frac{D_i T_o}{K_o^T}\right). \qquad (6)$$

Using this equation we can express the equilibrium constant of exchange.

$$\begin{cases} K_{eq} = \left(\dfrac{T_o D_i}{D_o T_i}\right)_{eq}, \\ \left(\dfrac{dD_i}{dt}\right)_{eq} = \left(\dfrac{dT_i}{dt}\right)_{eq} = \left(\dfrac{dD_o}{dt}\right)_{eq} = \left(\dfrac{dT_o}{dt}\right)_{eq} = 0. \end{cases}$$

From this it follows that

$$v'_{exchange} = \left(\frac{1}{\Delta'}\left(k_2 q\frac{T_i D_o}{K_o^D} - k_3\frac{D_i T_o}{K_o^T}\right)\right)_{eq} = 0,$$
$$K_{eq} = \left(\frac{T_o D_i}{D_o T_i}\right)_{eq} = q\frac{k_2 K_o^T}{k_3 K_o^D}. \qquad (7)$$

Using this equation we can express parameter q in terms of other parameters:

$$q = \frac{k_3 K_o^D}{k_2 K_o^T} K_{eq}, \qquad (8)$$

and then exclude it from Eq. 5.

Equations 5 and 6 include concentrations of the adenylates in their free deprotonated forms, which could be expressed in terms of total adenylate concentrations. By applying the equilibrium relationships for complex formation of adenine nucleotides with magnesium and proton ions, and relationships setting the total concentration of adenylates to the sum of concentrations of their different forms, we have expressed concentrations of free adenylates in terms of their total concentrations:

$$T = T_{total}\left(1 + \frac{Mg}{K_{Mg}^T} + \frac{H}{K_H^T} + \frac{Mg\,H}{K_{Mg}^{TH} K_H^T}\right)^{-1},$$
$$D = D_{total}\left(1 + \frac{Mg}{K_{Mg}^D} + \frac{H}{K_H^D} + \frac{Mg\,H}{K_{Mg}^{DH} K_H^D}\right)^{-1}.$$

Here, Mg and H are concentrations of free magnesium and proton ions, respectively. K_{Mg}^T, K_H^T, K_{Mg}^{TH}, K_{Mg}^D, K_H^D, K_{Mg}^{DH} are dissociation constants of proton/magnesium and adenylates. The values of these constants have been taken from Alberty's article (19).

Dependence of kinetic parameters on membrane potential

The transmembrane transfer of the adenylates depends on the electrostatic field of the charged membrane. To take this dependency into account we assume that kinetic parameters characterizing ANT function (rate and dissociation constants)

depend on membrane potential which, in its turn, unambiguously determines the electrostatic field of the charged membrane. We have developed a method enabling us to derive the dependencies of the parameters on membrane potential. In the framework of the method we assume that the total value of the membrane potential is the sum of ''local'' electric potentials and each of the ''local'' potentials influences the corresponding stage of the ANT catalytic cycle. To express these influences in terms of dependencies of kinetic constants of the stages of catalytic cycle on the corresponding ''local'' electric potentials we use well-known laws of thermodynamics, electrostatics, and the superposition rule.

Every position of the adenylate can be characterized by an electric potential value. In accordance with superposition rule, the sum of potential differences between the consecutive adenylate positions is equal to the total potential difference across the membrane. We have assumed that the difference in potentials between the adjacent positions of an adenylate is proportional to the total potential difference across the membrane. The applied approach divides the drop in potentials into elementary stages. We have described the influence of the electric field on them in terms of the drop in potential at each stage. The scheme depicted in Fig. 3 illustrates the influence of the potential on the rate of the antiporter operation. Values of the potential drop are marked for all stages of the scheme. We have applied the Nernst equation to derive the dependence of the equilibrium constant of ANT-catalyzed ADP/ATP exchange on potential. Since ATP/ADP exchange has a 1:1 stoichiometry and, consequently, results in transfer of only one elementary charge across the membrane, we obtain

$$K_{eq} = \exp(\phi), \phi = F\varphi/RT, K_{eq}(0) = 1,$$

where φ is the potential difference across the membrane. (From here on we use the dimensionless quantity of potential ϕ.)

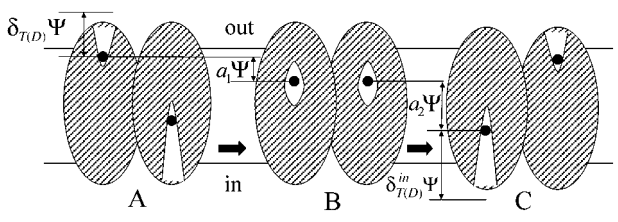

FIGURE 3 Scheme of ANT used to derive the dependence of the transfer rate on the electrostatic membrane potential. (*A–C*) Consecutive states of the ANT functional unit in the process of adenylate translocation. $\delta_{T(D)}$ is the ratio of the potential difference between the adenylate bound at the site of ANT facing the external side of the membrane and adenylate in the bulk phase to the total membrane potential, $\delta^{in}_{T(D)}$ is the ratio of the potential difference between the adenylate bound at the site of ANT facing the internal side of the membrane and adenylate in the bulk phase to the total membrane potential, a_1 is the displacement of the external adenylate from the coordinate of the maximum of the potential barrier, and a_2 is the displacement of the internal adenylate from the coordinate of the maximum of the potential barrier.

The dependence of the dissociation constant of binding of the external ATP to the free form of ANT upon the potential can be evaluated using the Nernst equation for each equilibrium stage:

$$\Delta\bar{\mu} = \Delta\bar{\mu}_0 - 4F\delta\varphi + RT\ln\{T_o \cdot E/(TE)\} = 0,$$

and then

$$K_o^T = (T_o E/ET)_{eq} = K_o^{T,0}\exp(4F\delta_T\varphi/RT) = K_o^{T,0}\exp(4\delta_T\phi),$$

$$K_o^{T,0} = K_o^T(\phi = 0), \tag{9}$$

where $\delta_T = \Delta\varphi/\varphi$ is the ratio of the potential difference between the ATP binding site and the space outside the membrane to the total membrane potential; -4 is the ATP charge in terms of elementary charges. We have assumed that δ_T is a constant value. Similarly, we have derived a potential dependence of the dissociation constant of binding of the external ADP to the free form of ANT:

$$K_o^D = K_o^{D,0}\exp(3\delta_D\phi), \quad K_o^{D,0} = K_o^D(\phi = 0). \tag{10}$$

The influence of potential on the transfer constants could be accounted for using Eyring's theory of absolute reaction rates. We have assumed that the energy profile of the transfer across the membrane (limiting stage) is a single barrier (Fig. 4), and the transfer is a jump over the barrier from one potential well to another. We have defined the reaction coordinate as the coordinate of adenylate bound to the inner side along its transfer direction across the membrane. In this case, the transport rate is determined by the probability of the system to transfer to this or another stage and depends on the

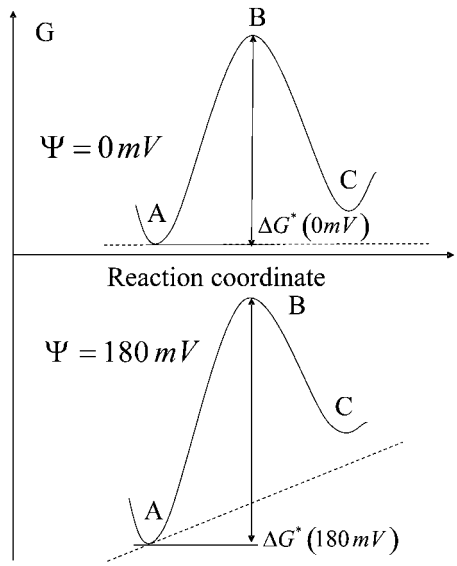

FIGURE 4 Potential barrier profile used to derive the dependence of the rate upon the membrane potential along the reaction coordinate. The dashed line shows the profile of the potential created by the field of the charged membrane. *A, B,* and *C* correspond to the ANT states depicted in Fig. 3.

barrier's height. The *A* and *C* states (Fig. 3) refer to the ANT bound with adenylates and ready to proceed with turnover. Stage *B* refers to the maximum of the potential barrier during the transfer process. In the general case, where the free energy has different profiles for different types of exchange (ATP for ATP, ADP for ADP, and ATP for ADP), we take into consideration different values of the rate constants and charges of the transported molecules.

If the potential increases, the parameters of the energy profile change as well (Fig. 4), which induces a change of the transfer constants:

$$k \sim \exp\{-\Delta G^*/(RT)\}, \tag{11}$$

where ΔG^* is the value of the energy barrier.

If the membrane potential is not zero, the height of the energy barrier is determined by the interactions of the membrane's electrostatic field with charges of the enzyme and adenylates bound, i.e., it depends on their displacement in the process of transfer from stage *A* to stage *C*. Assuming the additivity of the energy of interactions between these charges, the free energy, and the field of the charged membrane, the activation energy of charges Z_j displaced for the distance δ_j in the process of transfer from stage *A* into stage *C* can be expressed as

$$\Delta G^* = \Delta G_0^* + F\varphi\sum Z_j\delta_j.$$

In our case,

$$\Delta G^* = \Delta G_o^* + F\varphi(Z_1a_1 + Z_2a_2 + a_3), \tag{12}$$

where a_1 is the displacement of the external adenylate to the maximum coordinate, a_2 is the displacement of the internal adenylate, $a_3 = \sum Z_k\delta_k$ is the effective parameter characterizing the displacement of all charges of the enzyme.

By using Eqs. 11 and 12, we obtain

$$k_i = k_i^0 \exp(Z_1a_1\phi + Z_2a_2\phi + a_3\phi),$$

$$k_i^0 = k_i|_{\phi=0}, i = 1..4. \tag{13}$$

The potential drop $\delta^{in}_{T(D)}$ resulting from the adenylate dissociation/binding from/with the matrix site of ANT is not independent and is expressed in terms of other potential drops:

$$\delta^{in}_{T(D)} = 1 - \delta_{T(D)} - a_1 - a_2.$$

This parameter has been already taken into account in the equation expressing the dependence of the equilibrium constant of ATP/ADP exchange on electric potential difference and, consequently, there is no need to use it again.

Estimation of parameters

As was mentioned above, to verify a quantitative model it is necessary to identify its kinetic parameters by fitting experimental results. As a criterion of fitness, the following function was used:

$$f(k_j, K_j) = \sum_i^n (v_i - \hat{v}_i)^2. \tag{14}$$

Here, *n* is the total number of the experimental points, $\hat{v}_i$ is the experimentally measured value of the influx rate (10), v_i is the value of the influx rate calculated on the basis of the model at a point corresponding to the experimental ones. To estimate values of unknown parameters the absolute error of the model ($\sqrt{f}$) has been minimized. This procedure was performed in the DBSolve 7.01 package (20) using the Hook-Jeeves method (21). We have identified two sets of the kinetic parameters for two series of the experiments (with or without the membrane potential). Parameter values are shown in Table 1.

Using Eqs. 9, 10, and 13, we have derived a system of algebraic equations giving the parameters characterizing potential dependence of the ANT operation as functions of the parameters whose values were estimated against experimental data and summarized in Table 1:

$$\begin{cases} \exp\{((-4)a_1 + (-4)a_2 + a_3)6.9\} = k_1^{6.9}/k_1^0, \\ \exp\{((-3)a_1 + (-4)a_2 + a_3)6.9\} = k_2^{6.9}/k_2^0, \\ \exp\{((-4)a_1 + (-3)a_2 + a_3)6.9\} = k_3^{6.9}/k_3^0, \\ \exp\{4\delta_T 6.9\} = K_o^{T,6.9}/K_o^{T,0}, \\ \exp\{3\delta_T 6.9\} = K_o^{D,6.9}/K_o^{D,0}. \end{cases}$$

Solving the system, we have obtained the following values of the unknown parameters: $a_1 = -0.268$, $a_2 = 0.205$, $a_3 = 0.187$, $\delta_T = 0.07$, $\delta_D = 0$. It is worth noting that these values are approximate. Their accuracy is affected by the tolerance of the numerical evaluation, and of the precision of the experimental techniques.

RESULTS

As described in the previous section, we have found two sets of kinetic parameters that correspond to two sets of experimental data (in the presence and absence of the membrane potential). Using Eqs. 9, 10, and 13, we can identify a single set of parameters (Table 2) that fits all experimental points

TABLE 1 Values of the apparent kinetic parameters calculated on the basis of two sets of the experimental data measured at $\Psi = 0$ mV and $\Psi = 180$ mV

Parameter	$\Psi = 0$ mV	$\Psi = 180$ mV
k_1	35 min^{-1}	22 min^{-1}
k_2	10.8 min^{-1}	44 min^{-1}
k_3	21 min^{-1}	3.4 min^{-1}
k_4	29 min^{-1}	29 min^{-1}
K_o^D	51 μM	51 μM
K_o^T	57 μM	393 μM
K_i^D/K_i^{T*}	1.8	9.7

*Dependent parameter (can be expressed from other parameters).

TABLE 2 Values of parameters of the model and ranges of sensitivity

Parameter	Value	Range of sensitivity
k_1^0	35 min^{-1}	(31–39) min^{-1}
k_2^0	10.8 min^{-1}	(10.1–11.6) min^{-1}
k_3^0	21 min^{-1}	(13–43) min^{-1}
k_4^0	29 min^{-1}	(26–32) min^{-1}
$K_o^{D,0}$	51 μM	(45–57) μM
$K_o^{T,0}$	57 μM	(45–71) μM
a_1	−0.268	−(0.265–0.271)
a_2	0.205	(0.203–0.207)
a_3	0.187	(0.179–0.196)
δ_T	0.07	(0.06–0.09)
δ_D	0.000	(0.000–0.006)

(10). Both the theoretical simulations and the experimental data are depicted in Fig. 5.

Since the rate equation (Eq. 5) is a nonlinear function it has different sensitivity with respect to different parameters. This means that the accuracy of parameter estimation differs as well. To study sensitivity of the model solution we varied each parameter individually, calculated the discrepancy of the model (f) and found a range of the parameter values providing no more than a twofold increase in the f value (see Table 2).

Based on results shown in Tables 1 and 2, we can conclude that ~7% of the electric potential is lost at the ATP binding stage. The binding constant for the external ATP depends to a significant degree upon the potential. Indeed, variation of the electric potential from 0 to 180 mV results in ~60% increase in the value of K_o^T. In contrast, we have not detected a dependence of K_o^D on electric potential. However, because of low sensitivity of the solution with respect to δ_D, this conclusion is questionable, so additional experimental data are needed.

Deviations of the values of the parameters a_1 and a_2 from zero imply that changes in the conformation of the dimer of ANT result in significant changes in the positions of the adenylates. The value of 0.187 for the parameter a_3 indicates the presence of charged groups on the surface of the ANT molecule that shift during the adenylate transfer.

The model was applied to study the antiporter behavior under close-to-physiological conditions. The theoretical dependencies depicted in Fig. 6 have been calculated by using concentration values of the metabolites equal to those in mitochondria.

Under uncoupled conditions, the model predicts ADP efflux out of mitochondria (negative values of the exchange velocities in Fig. 6 *A*). This is mainly due to dependence of the equilibrium constant of the ADP/ATP exchange upon the potential. During the energization of mitochondria, the positive direction of the transfer is maintained even under very low concentrations of external ADP. The transfer results in the accumulation of ADP in the mitochondrial matrix. This stimulates the increase in the rate of ATP synthesis in mitochondria. Fig. 6 *B* shows the dependence of the exchange

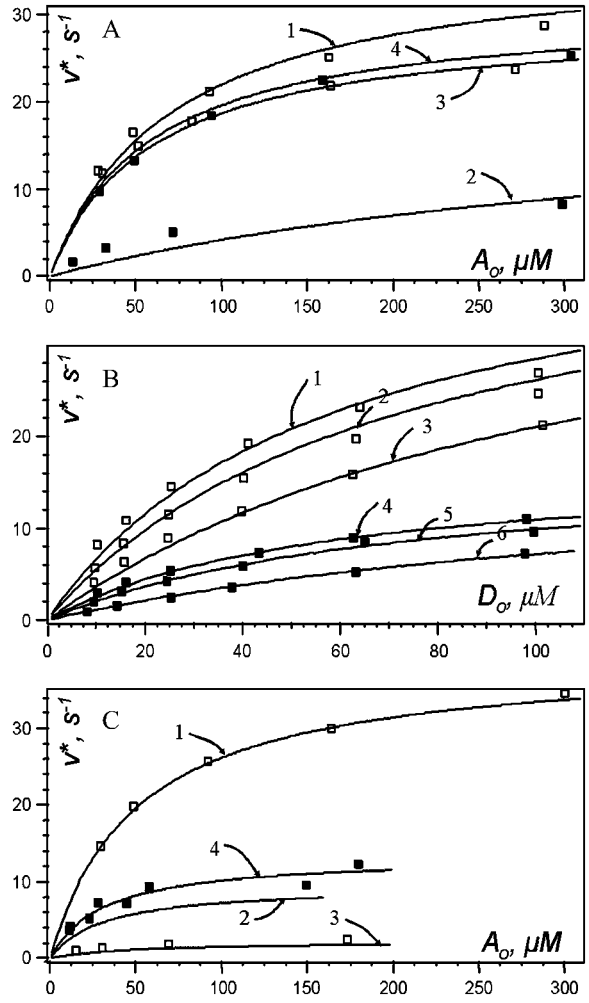

FIGURE 5 Results of parameter estimation. The experimental values (*symbols*) taken from Kraemer and Klingenberg (10) and model-generated curves (*solid lines*), at pH 8.0, $Mg^{2+} = 0$ are shown. (*A*) The dependence of influx rate of the labeled adenylate (v^*) on: 1), the concentration of the external labeled ATP ($T_i = 10$ mM, $D_i = 0$ mM, $D_o = 0\,\mu$M, $\Psi = 180$ mM); 2), the concentration of the external labeled ATP ($T_i = 10$ mM, $D_i = 0$ mM, $D_o = 0\,\mu$M, $\Psi = 0$ mM); 3), the concentration of the external labeled ADP ($T_i = 0$ mM, $D_i = 10$ mM, $T_o = 0\,\mu$M, $\Psi = 180$ mV); and 4), the concentration of the external labeled ADP ($T_i = 0$ mM, $D_i = 10$ mM, $T_o = 0\,\mu$M, $\Psi = 0$ mV). (*B*) The dependence of influx rate of the labeled adenylate (v^*) on the concentration of the external labeled ADP: 1), $T_i = 5$ mM, $D_i = 5$ mM, $T_o = 0\,\mu$M, $\Psi = 180$ mV; 2), $T_i = 5$ mM, $D_i = 5$ mM, $T_o = 100\,\mu$M, $\Psi = 180$ mV; 3), $T_i = 5$ mM, $D_i = 5$ mM, $T_o = 400\,\mu$M, $\Psi = 180$ mV; 4), $T_i = 5$ mM, $D_i = 5$ mM, $T_o = 0\,\mu$M, $\Psi = 0$ mV; 5), $T_i = 5$ mM, $D_i = 5$ mM, $T_o = 20\,\mu$M, $\Psi = 0$ mV; and 6), $T_i = 5$ mM, $D_i = 5$ mM, $T_o = 100\,\mu$M, $\Psi = 0$ mV. (*C*) The dependence of influx rate of the labeled adenylate (v^*) on: 1), the concentration of the external labeled ADP ($T_i = 5$ mM, $D_i = 5$ mM, $T_o^* = D_o^*$, $\Psi = 180$ mV); 2), the concentration of the external labeled ADP ($T_i = 5$ mM, $D_i = 5$ mM, $T_o^* = D_o^*$, $\Psi = 0$ mV); 3), the concentration of the external labeled ATP ($T_i = 5$ mM, $D_i = 5$ mM, $D_o^* = T_o^*$, $\Psi = 180$ mV); and 4), the concentration of the external labeled ATP ($T_i = 5$ mM, $D_i = 5$ mM, $D_o^* = T_o^*$, $\Psi = 0$ mV).

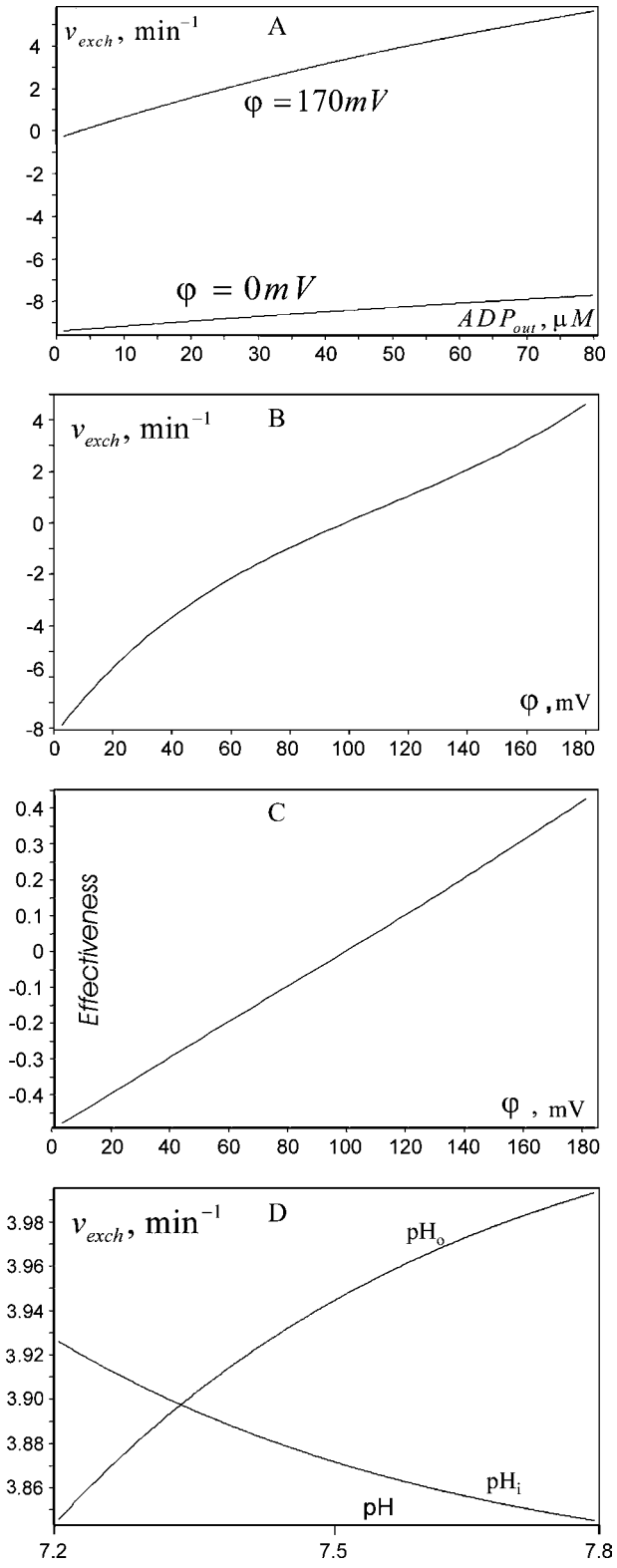

FIGURE 6 (*A*) Calculated dependence of the ATP/ADP exchange rate upon concentration of the external ADP at various fixed values of the membrane potential. $pH_i = 7.8, pH_o = 7.2, Mg^{2+} = 1\,mM, T_i = D_i = 5\,mM, T_o = 2\,mM$. (*B*) The calculated dependence of the ATP/ADP exchange rate upon the membrane potential. Parameter values: $pH_i = 7.8$, $pH_o = 7.2, Mg^{2+} = 1\,mM, T_i = D_i = 5\,mM, T_o = 2\,mM$, $D_o = 50\,\mu M$. (*C*) The calculated dependence of the ATP/ADP exchange ''effectiveness'' (ratio of exchange rate to the total number of turnovers) upon the membrane potential. Parameter values: $pH_i = 7.8$, $pH_o = 7.2, Mg^{2+} = 1\,mM, T_i = D_i = 5\,mM, T_o = 2\,mM, D_o = 50\,\mu M$. (*D*) The calculated dependence of the ATP/ADP exchange rate upon pH inside and outside mitochondria. Each curve involves the change of the pH values in one of the compartments relative to the fixed pH in the other one. Parameter values: $pH_i = 7.8$, $pH_o = 7.2$, $Mg^{2+} = 1\,mM, T_i = D_i = 5\,mM$, $T_o = 2\,mM, D_o = 50\,\mu M, \varphi = 170\,mV$.

rate upon the potential. It has a positive direction only at potentials not less than 100 mV.

To characterize the effectiveness of the antiporter operation we have introduced a new function: the ratio of the exchange rate to the total turnover number per time unit.

$$\text{effectiveness} = v'_{\text{exchange}}/v'.$$

This function relates changes in ADP concentration in the mitochondrial matrix to the total number of ANT transfer cycles. The dependence of the effectiveness upon the membrane potential is shown in Fig. 6 *C*. The negative values of the effectiveness indicate the opposite transfer direction. Within the given range of the parameters, the effectiveness of the transfer is not more than 0.5, even for energized mitochondria. This means that no more than half of the transfer cycles result in an outward ATP flux. This can be explained by a low concentration of external ADP because the probability of the complex forming with ADP from the intramembrane space is lower than with ATP.

To describe the processes of the adenylate protonation/deprotonation, we have assumed that only free forms of the adenylates can be transferred by ANT across the membrane, and the affinity of ADP to ANT binding sites differs significantly from that of ATP. The changes in internal and external pH cause a change in the ratio of the free forms of ADP and ATP and, consequently, the exchange rate. Fig. 6 *D* shows that the exchange rate increases with the increase of external pH and decreases with the increase of internal pH. It is worth mentioning that to describe ANT function properly the model has to take into account the pH dependence of both adenylate distributions between free and protonated forms and the ability of ANT to transfer bound adenylates across the membrane. To quantify the pH dependence of ANT activity, additional experimental data are required.

DISCUSSION

In this study, we have used what we believe is all available experimental information about adenine nucleotide translocase to develop a predictive model explaining the physical and kinetic peculiarities of ANT function. Two possible mechanisms of ANT function have been suggested on the basis of available structural and kinetic information. These

two mechanisms correspond to two possible types (*cis* or *trans*) of subunit composition in the ANT homodimer. In accordance with data obtained in experiments analyzing inhibition, we have found that the composition of subunits in the functional unit of ANT is the *cis* type. The distinctive feature of the mechanism of ANT function based on the *cis*-type subunit composition is the presence of unique types of binding site on each side of membrane. In terms of enzyme kinetics this means that the affinity of adenylates with respect to ANT binding sites pointing toward both compartments (mitochondrial matrix or intermembrane space) does not depend on the conformations of the functional unit.

A kinetic scheme of the ANT catalytic cycle has been developed (see Fig. 2) based on the *cis*-mechanism of ANT function. The scheme represents a set of ANT states interconnected by elementary reactions involved in adenylate translocation. The kinetic scheme has been built on the basis of the following principle: one action in the functional mechanism corresponds to one reaction of the kinetic scheme. This scheme includes all types of adenylate exchanges (both productive and futile cycles), and implies that the binding of adenylates is independent. The question about cooperativity of adenylate binding remains open because of lack of experimental data. As a result, we have assumed the simplest case to construct the kinetic model. This implies that the dissociation constant of adenylate is independent of binding on the opposite site. Otherwise, the model would have many more free parameters without improvement in the fitting of the results.

Applying quasi-steady-state and quasi-equilibrium approaches to the kinetic scheme, we have derived the rate equations describing total turnover of ATP and ADP influx (Eqs. 5 and 6). For kinetic parameter estimation we have used the procedure of fitting described above. The parameters have been fitted to minimize the discrepancy between experimental data and calculated dependencies. It is necessary to note that the algorithm applied does not generate a unique set of the parameter values. This is because there are no numerical methods to calculate the global minimum in multiparameter space. One of the possible ways to examine the system for the existence of other solutions is to apply the fitting procedure starting from various initial points in parameter space. We have done it eight times and all solutions are coincident with each other. This can be considered as indirect confirmation of the uniqueness of the solution.

Since the antiporter behavior depends significantly upon the electric field across the membrane, we have described the features of ANT function in terms of the dependence of the kinetic parameters on electric potential difference. We have analyzed two ways of introducing this dependence into the model: either via the affinity of the adenylates or through the transfer rate (data not shown). We have found that assuming that both the affinity constants and the rate constants are dependent on the potential results in the best coincidence between experimental data and the model-generated curves (see Table 1). Aliev and Saks (5) described similar findings. As an additional constraint on the parameter values we have used an equilibrium constant determined in accordance with the Nernst equation. The value of the constant has been calculated on the basis of a 1:1 stoichiometry and is in good agreement with that in the work of Klingenberg (9).

An increase in membrane potential (Table 1) results in an increased affinity of the ANT binding site facing the matrix, and a decreased affinity of the binding site facing the intermembrane space with respect to ATP, thus maintaining the direct adenylate exchange (ATP leaves the matrix).

Sensitivity analysis of the parameters (see Table 2) has been carried out. The results demonstrate that the following parameters δ_T, δ_D, k_3^o, and K_o^T influence the fitting results weakly, and hence additional experimental data are required to estimate them more precisely. Furthermore, the available experimental data (10) do not allow us to estimate absolute values of inner dissociation constants of adenylates, but only their ratio. Additional experiments with low adenylate concentrations would be helpful.

The quality of the model fit against experimental data is illustrated by Fig. 5. It is interesting to compare our model to other ones. The logarithmic Akaike Information Criterion has been chosen for the comparison

$$AIC = \ln(\langle s^2\rangle/n) + 2k/n,$$

$$\langle s^2\rangle = \sum_i^n \left(\frac{v_i - \hat{v}_i}{\hat{v}_i}\right)^2.$$

This criterion is usually used to choose the optimal model from a number of different models simulating a set (with n experimental points) of experimental data. It depends not only on the relative discrepancy value ($\langle s^2\rangle$), but also on the number of parameters in the model (k parameters). Table 3 shows that in frameworks of both relative error and AIC criterion the quality of the mathematical model developed in this article exceeds that of the models developed by Aliev and Saks (5) and Kraemer and Klingenberg (10).

The model allows us not only to simulate experimental data, but also to predict characteristics of ANT function that are difficult to measure experimentally. For example, we have calculated the dependence of the exchange rate on membrane potential and metabolite concentrations at physiological conditions. We have found that most of ANT turnovers

TABLE 3 Comparison of different models simulating experimental data (10)

Model	Number of experimental points	Number of parameters	Mean error $\sqrt{\langle s^2\rangle/n}$	AIC
Kraemer, Klingenberg (10)	24	9	0.30	−1.63
Aliev, Saks (5)	24	18	0.24	−1.39
Model developed in this article	72	11	0.23	−2.63

are futile even at a high potential value. We have also calculated how changes in internal and external pH influence exchange rate. It turned out that the exchange rate decreased slightly, whereas inner pH increased; this was previously shown experimentally by Klingenberg (9).

The authors are grateful to Vladimir P. Skulachev for criticism and discussion.

This research was supported by the program of the Russian Academy of Sciences ''Electronic Mitochondrion of the Yeast''.

REFERENCES

1. Kholodenko, B. N. 1984. Control of mitochondrial oxidative phosphorylation. *J. Theor. Biol.* 107:179–188.
2. Kholodenko, B. N. 1984. The mitochondrial carrier of adenylates controls ATP production in the physiological range of respiration rates. *Biofizika* (*Moscow*). 29:453–458.
3. Davis, E. J., and W. I. A. Davies-Van Thienen. 1984. Rate control of phosphorylation-coupled respiration by rat liver mitochondria. *Arch. Biochem. Biophys.* 233:573–581.
4. Kholodenko, B. N. 1988. Stabilizing regulation in polyenzyme systems: bioenergetic processes modeling. Ph.D. thesis, Moscow State University, Moscow, Russia.
5. Aliev, M. K., and V. A. Saks. 2003. Analysis of the mechanism of functioning of mitochondrial adenine nucleotide translocase using mathematical models. *Biofizika* (*Moscow*). 48:1075–1058.
6. Vignais, P. V., M. R. Block, F. Boulay, G. Brandolin, and G. L. M. Lauquin. 1982. Functional and topological aspects of the mitochondrial adenine-nucleotide carrier. *In* Membranes and Transport, Vol. 1 A. N. Martonosi, editor. Plenum Press, New York. 405–414.
7. Vignais, P. V., M. R. Block, F. Boulay, G. Brandolin, and G. L. M. Lauquin. 1985. Molecular aspects of structure-function relationships in mitochondrial adenine nucleotide carrier. *In* Structure and Properties of Cell Membranes. V. Benga, editor. CRC Press, Paris. 139–179.
8. Klingenberg, M. 1980. The ADP-ATP translocation in mitochondria, a membrane potential controlled transport. *J. Membr. Biol.* 56:97–105.
9. Klingenberg, M., and H. Rottenberg. 1977. Relation between the gradient of the ATP/ADP ratio and the membrane potential across the mitochondrial membrane. *Eur. J. Biochem.* 73:125–130.
10. Kraemer, R., and M. Klingenberg. 1982. Electrophoretic control of reconstituted adenine nucleotide translocation. *Biochemistry.* 21:1082–1089.
11. Cleland, W. W. 1963. The kinetics of enzyme-catalyzed reactions with two or more substrates or products. *Biochim. Biophys. Acta.* 67:104–137.
12. Duyckaerts, C., C. M. Sluse-Goffart, J. P. Fux, F. E. Sluse, and C. Liebecq. 1980. Kinetic mechanism of the exchanges catalysed by the adenine-nucleotide carrier. *Eur. J. Biochem.* 106:1–6.
13. Barbour, R. L., and S. H. P. Chan. 1981. Characterization of the kinetics and mechanism of the mitochondrial ADP-ATP carrier. *J. Biol. Chem.* 256:1940–1948.
14. Brandolin, G., J. Doussiere, A. Gulik, T. Gulik-Krzywicki, G. J. M. Lauquin, and P. V. Vignais. 1980. Kinetic, binding and ultrastructural properties of the beef heart adenine nucleotide carrier protein after incorporation into phospholipid vesicles. *Biochim. Biophys. Acta.* 592: 592–614.
15. Pebay-Peyroula, E., C. Dahout-Gonzalez, R. Kahn, V. Trezeguet, G. J. M. Lauquin, and G. Brandolin. 2003. Structure of mitochondrial ADP/ATP carrier in complex with carboxyatractyloside. *Nature.* 426:39–44.
16. Demin, O. V., H. V. Westerhoff, and B. N. Kholodenko. 1998. Mathematical modelling of superoxide generation with the bc1 complex of mitochondria. *Biochemistry* (*Moscow*). 63:634–649.
17. Demin, O. V., I. I. Goryanin, B. N. Kholodenko, and H. V. Westerhoff. 2001. Kinetic modeling of energy metabolism and generation of active forms of oxygen in hepatocyte mitochondria. *Mol. Biol.* (*Moscow*). 35:1095–1104.
18. Pfaff, E., H. W. Heldt, and M. Klingenberg. 1969. Adenine nucleotide translocation of mitochondria: kinetics of the adenine nucleotide exchange. *Eur. J. Biochem.* 10:484–493.
19. Alberty, R. A. 1992. Equilibrium calculations on systems of biochemical reactions at specified pH and pMg. *Biophys. Chem.* 42:117–131.
20. Goryanin, I., T. C. Hodgman, and E. Selkov. 1999. Mathematical simulation and analysis of cellular metabolism and regulation. *Bioinformatics.* 15:749–758.
21. Hook, R., and T. A. Jeeves. 1961. ''Direct search'' solution of numerical and statistical problems. *J. ACM.* 8:212–229.